Modeling of Whale Optimization with Deep Learning based Brain Disorder Detection and Classification

Uvaneshwari M[1], Dr. M. Baskar[2]*
Research Scholar-Department of Computer Science and Engineering-School of Computing-College of Engineering and Technology, SRM Institute of Science and Technology, Kattankulathur, Chengalpattu, Tamilnadu, 603 203, India[1]
Associate Professor-Department of Computing Technologies-School of Computing-College of Engineering and Technology, SRM Institute of Science and Technology, Kattankulathur, Chengalpattu, Tamilnadu, 603 203, India[2]

***Abstract*—Brain disorders are a significant source of economic strain and unfathomable suffering in modern society. Imaging techniques help diagnose, monitor and treat mental health, neurological, and developmental disorders. To aid in the Computer-Aided Diagnosis of brain diseases, deep learning (DL) was used for the analysis of neuroimages from modalities including Positron Emission Tomography (PET), Structural Magnetic Resonance Imaging (SMRI), and functional MRI. In this study, a Whale Optimization Algorithm is used with Deep Learning to analyse MRI scans for signs of neurological disease. WOADL-BDDC may detect and label abnormalities in the brain based on an MRI scan. It uses a two-step pre-processing procedure, first using guided filtering to get rid of background noise and then using U-Net segmentation to get rid of the top of the head. QuickNAT, along with RMSProp, is used to segment the brain. When analysing data, WOADL-BDDC uses radionics to collect information from every layer. When used in a convolutional recurrent neural network model, the Whale Optimization Algorithm may accurately categorize mental illness. WOADL-BDDC is put through its paces using ADNI 3D. Compared to state-of-the-art classification results from Vgg16, Graph CNN, Modified ResNet18, Non-linear SVM, ResNet50-SVM, ResNet50-RF, the suggested technique achieved the greatest accuracy. It was demonstrated that the suggested model is superior to other models for classification from MRI images. In simulations, the proposed approach is shown to be effective in optimizing hyperparameters with an accuracy of 94.38 % on TR set and 94.87% on TS set, Precision of 96.43% on TR set and 97.62% on TS set, and an F1-Score of 89.35 % and 92.10% on TR and TS set, respectively.**

Keywords*—Brain disorder detection; magnetic resonance imaging; deep learning; convolutional recurrent neural network; whale optimization algorithm

I. INTRODUCTION

The brain is the management center of the central nervous system and is liable for implementing activities all over the human body [1, 2]. As in other medical sectors, there exist Innovative neuroimaging technologies comprising positron emission tomography (PET), and MRI was introduced and utilized for identifying Alzheimer's Disease (AD) based molecular and structural biomarkers [3,17]. Rapid progression in neuroimaging techniques makes them challenging to incorporate largescale, higher-dimension multimodal neuroimaging datasets [4]. Thus, computer-aided machine learning (ML) algorithms for integrative analysis have gained considerable interest. To apply this ML approach,Pre-Processing steps or appropriate architectural design must be defined in advance [5]. Generally, a classification study using the ML method needs four stages: feature selection, feature extraction, feature-based classification algorithm selection, and dimensionality reduction [6]. This process requires multiple optimization steps and professional knowledge that might take considerable time [7]. To conquer this problem, deep learning (DL), an emerging field of ML study that uses raw neuroimaging information to generate features through "on-the-fly" learning, is received significant interest in the Area of large-scale, higher-dimension medical imaging analysis. DL approaches, like convolution neural networks (CNN), have proved to outperform the present ML method [8, 9]. Compared with conventional ML techniques, the DL approach automatically discovers the proper representation without specialized knowledge and permits the non-expert to utilize DL approaches efficiently. Thus, the DL method has rapidly become a method of choice for medical image analysis [10].

This study progresses a Whale Optimization Algorithm with Deep Learning based Brain Disorder Detection and Classification (WOADL-BDDC) on MRI images. The WOADL-BDDC technique initially performs pre-processing in 2 stages: guided filtering (GF) based noise elimination and U-Net segmentation-based skull stripping. Besides, the QuickNAT with RMSProp optimizer is applied to segment the brain parts. For feature extraction, the WOADL-BDDC technique performs a radionics approach that separates features of all aspects. Finally, the WOA with convolutional recurrent neural network (CRNN) model is applied to classify brain disorders. The experimental evaluation of the WOADL-BDDC technique is tested on the ADNI 3D dataset.

The wide range in tumour size, shape, and location poses a significant problem for diagnosing brain tumours. The scientific community can benefit from this review since it provides a thorough literature on brain tumour detection using magnetic resonance imaging. The healthcare sector is unlike any other. Regardless of financial constraints, this is a top priority area that attracts customers expecting only the best service. Given deep learning's track record of success in the real world, it should be no surprise that this promising technique is already playing a crucial role in medical imaging, yielding promising results with high accuracy. The brain is the master organ, regulating the functions of every other body component.

*Corresponding Author.

Due to the intricacy of size and position variations, automated brain tumour recognition in MRI is challenging. The pictures produced from MRI scans of the brain are processed using proposed statistical, morphological, and thresholding methods to detect tumours.Based on our findings, we can confidently state that conventional algorithms perform admirably for both the number of initial clusters and the locations of their centers. Pixel classification becomes difficult if these groups shift depending on the parameters you use to construct them. As it is, the cluster centroid value is chosen at random in the most common fuzzy cluster mean procedure. Because of this, it will take longer to get the intended result. Radiologists have to spend a lot of time manually segmenting and evaluating MRI brain pictures. The segmentation is performed using machine learning approaches that are less accurate and have a slower calculation speed. Tumor categorization and identification using neural network methods have been attempted extensively but with mixed results. Detection accuracy relies on the segmentation and detection algorithms employed. Thus far, current systems need to provide better picture quality and precision.

A convolutional recurrent neural network (CRNN) will be employed to categorize the tumors in the picture. Increased precision and decreased repetition are the only two benefits of this method.

II. Literature Review

The authors [11] modeled a deep ensemble learning structure to harness DL techniques to tap the 'wisdom of experts' and compile multisource data. At the voting layer, two sparse AEs were instructed for feature learning to minimize the correlation of features and expand the base classifier eventually. At the stacking layer, a non-linear feature-weighted technique related to a DBN was devised to rank the base classifiers, which disrupt the conditional independence. In [12], the authors intend to formulate an innovative DL technique for detecting or productively predicting AD. The authors devised densely connected CNNs with a connection-wise attention system for learning the multilevel attributes of brain MRI for AD categorization. The authors employed the densely associated NN for deriving multiscale features in pre-processing images. A connection-wise attention system has been implemented for integrating associations among attributes from distinct layers. In [13], the authors employ a DL-related Granger causality estimation of brain connectivity structure. It uses the robustness of LSTM in changing time series processing. The authors employ MRI to examine the cerebral cortex property and exploit rs-fMRI to analyze the function network's graph metric. In [14], the authors establish that it is settled well with the multi-task learning method. In [15] devised a DL technique for every level of feature extracting process and fuzzy hyper-plane related least square twin SVM (FLS-TWSVM) for classifying the derived features for initial analysis of AD through removing sagittal plane slices from 3-D MRI imageries. In [16], an Alzheimer's classification and detection method was provided. The BoVW method was employed to enhance the efficacy of texture-related features, like the histogram of gradient, GLCM, and scale-invariant feature transform, LBP.

Brain tumours are notoriously difficult to diagnose because of the wide range of tumour sizes, forms, and shapes that must be considered during the process [25]. Surgical, radiological, and chemotherapeutic options are all on the table when a brain tumour diagnosis has been made, and prognoses can be formulated based on the tumor's nature and location [26]. Therefore, early diagnosis and identification of brain tumours aid in treatment planning and patient monitoring. It's a vital factor in better treatment and increased survival rates. To learn more about tumours, many medical imaging and diagnostic methods are performed. It is possible to distinguish between usually and abnormally expanding brain cells with the aid of imaging techniques like magnetic resonance imaging (MRI) and computed tomography (CT)[27]. Computed Tomography (CT) scans are utilized for diagnosis through X-ray and computer to produce pictures of the patient's brain in axial slices [28].

According to the systematic literature evaluation, there is space for improvement in brain tumour detection. Because brain tumours can be any size or shape, current segmentation methods need further work before they can be used for tumours. The importance of enhancement and segmentation in tumour identification stems from their role in addressing the shortcomings of current approaches.

The significance of medical data offered along with imaging data can be emphasized by incorporating clinical features, including texture-related features, for generating hybrid feature vectors. Though several computer-aided diagnosis models are existed in the literature to perform the brain tumor classification processes, it is required to improve the classifier results. Due to the repeated extension of the model, the number of parameters of DL models also rises rapidly, which leads to model overfitting. So, the WOA algorithm is used to select CRNN parameters. Personalized image collection based on estimates has been proven to be capable of seeing channels during a CT examination, thanks to the ongoing development of AI. Significant learning, in particular, has demonstrated encouraging outcomes in automated planning. It's so good at processing visual information that we can now employ neural connections to construct meaningful images rather than merely sort them. In particular, CRNN Association is well suited for evaluating images from channels like CT and X-ray. CRNNs are mainly designed to handle photographs better and finish picture groups. In this way, CRNNs can approach radiologists' accuracy when recognizing crucial elements in CT channels or other signature images.

III. The Proposed WOADL-BDDC Model

In this study, we have established a new WOADL-BDDC technique for recognizing brain disorders on MRI images. The WOADL-BDDC approach encompasses GF-based noise removal, U-Net-based skull stripping, QuickNAT with RMSProp-based brain segmentation, radionics feature extraction, CRNN classification, and WOA hyperparameter tuning. Fig. 1 represents the block diagram of the WOADL-BDDC system.

A. Image Pre-Processing

A GF is an edge-preserving smoothing light filter. It applies edge-preserving smoothing on the image, utilizing the content of the secondary image, named a guidance image, to impact the filtering. The guidance image could be a completely different image or different versions of an image. The bilateral filter might filter out texture or noise when maintaining sharp edges. A Gaussian operator can compute the convolution operator, and a proposal of Gaussian smoothening can be made by convolution. The Gaussian operator can be defined using the following equations:

$$G_{1D}(x) = \frac{1}{\sqrt{2\pi}\sigma} e^{-\left(\frac{x^2}{2\sigma^2}\right)} \quad (1)$$

The optimum smoothening filter for the image can be localized in the frequency and spatial domains, where the ambiguity relativity can be satisfied as follows [19]:

$$\Delta x \Delta \omega \geq \frac{1}{2}. \quad (2)$$

The Gaussian operator in 2D can be represented by:

$$G_{2D}(x, y) = \frac{1}{2\pi\sigma^2} e^{-\left(\frac{x^2+y^2}{2\sigma^2}\right)} \quad (3)$$

Where σ (sigma) signifies the standard deviation (SD) of Gaussian and(x, y) represents the Cartesian coordinates of the image. In medical applications, it serves as an initial phase since it identifies path abnormality in the speed, brain, and accuracy of diagnoses. It isolates non-brain tissues such as the scalp and skull from the brain image. Skull stripping removes unwanted components and non-brain anatomy from scanned images. There exist five convolution blocks in the downsampling route. Currently, there are overall of 1024 feature maps. Excepting the last block, max pooling with stride 22 can be performed after the completion of every block for downsampling. The feature map is reduced in size from 240x240 to 1515. Each up-sampling block initiates by a deconvolution layer of stride 22 and filters size 33. Consequently, feature map is becoming increasingly popular. The two convolution layers in the up-sampling block lower the quantity of deconvolution feature map and feature map in the encoding route.

B. Brain Segmentation

In this work, the QuickNAT carries out the segmentation of brain regions with RMSPropoptimizer.QuickNAT is the first method that uses an unlabelled neuroimaging dataset with auxiliary labels for training and a higher testing speed of the FC network for brain segmentation [18]. QuickNAT comprises sagittal, coronal, and axial views monitored by a view aggregation stage to deduce the last segment. Every FCNN is a similar structure and is stimulated by the conventional encoding/decoding-based UNet structure with skip connection improved with an un-pooling layer. Also, the study presents dense links in all the encoding/decoding blocks to promote feature re-usability and to help gradient flow, that is, the small number of training datasets. A multi-class Dice loss and weighted logistic loss can enhance the network.

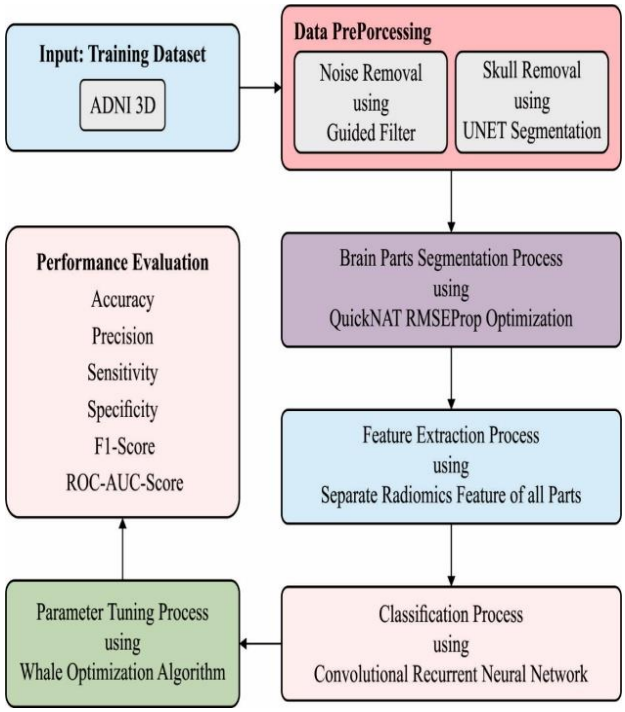

Fig. 1. Block diagram of WOADL-BDDC system.

In contrast, it compensates for higher-class imbalanced datasets and encourages the accurate assessment of anatomical boundaries using a proper weighting system. The two primary techniques of QuickNAT are the training method with auxiliary labels and the FCNN framework. The trained model and code are presented as extensions of MatConvNet for off-the-shelf usage.

C. Radiomics Feature Extraction

For the process of extracting features, the presented algorithm will use radionics features. The abovementioned features are derived by in-house software, utilizing PyRadiomics and python's skit-learn package [19]. Texture, intensity, and shape are the three kinds of features that are calculated. Twenty-six shape-based and intensity-based features can be extracted for all extraction settings (width, filter, bin, and contour). With sixteen distinct stages, which can be permutations of 2 contours (HGG and Gold), bandwidth (2, 4, 8, 16), and two filters (LoG and original) and the entire count of derived radionics imaging features was 1450.

D. CRNN-Based Brain Disorder Classification

The CRNN model is applied here to detect and classify brain disorders. The study presents the CRNN utilized for organizing MRI [20]. Initially, CNN is used for learning higher-level feature representation. Next, the CNN-learned feature was fed into the Bi-GRU layer for learning the temporal correlation data. At last, this feature was provided in the FC layer bySoftmax function for the outcome of the likelihood distribution of distinct classes. In the presented method, the convolution RNN has encompassed two BiGRU layers $(l_9 - l_{10})$ and eight convolution layers $(l_1 - l_8)$. The network parameter and architecture are given below:

$l_1 - l_2$: The first two stacked convolution layer uses 32 filters with the stride of (1,1) and receptive field of (3,5). Then, max-pooling with the stride of (4,3) decreases the size of feature maps.

$l_3 - l_4$: The subsequent two convolution layers use 64 filters with a stride of (1,1) and a receptive field of (3,1) and are utilized for learning local patterns alongside the frequency dimension. It can be max-pooling with the stride of (4,1).

$l_5 - l_6$: The succeeding pairs of convolution layer applied 128 filters with a stride of (1,1) and receptive field of (1,5) and are utilized for learning local patterns along the time dimension. It can subsequently be the max-pooling with the stride of (1,3).

$l_7 - l_8$: The successive two convolution layer uses 256 filters with a stride of (1,1) and receptive field of (3,3) for learning joint time–frequency features. It can subsequently be the max-pooling of (2,2) stride.

$l_9 - l_{10}$: 2BiGRU layers with 256 cells were utilized for temporal summarization, and the activation function was used. The dropout with the possibility of 0:5 is applied to every Bi-GRU layer to prevent over-fitting. Fig. 2 illustrates the framework of CRNN.

E. Hyperparameter Tuning

For adjusting the hyperparameters related to the CRNN model, the WOA is utilized in this work. WOA is a population-based heuristic approach that models the hunting strategy of humpback whales [21]. They construct unique maneuvers for paralyzing the prey by swimming nearby them in a spiral or circle-shaped path. This technique is named the bubble-net attack. The hunting behavior can be specified into two stages. The initial stage is the exploration phase, where the whales randomly seek prey. The next stage is the exploitation stage, whereby the whales implement bubble-net hunting. The following equation is utilized for mathematically modeling these behaviors as follows:

$$\vec{D} = \left|\vec{C}.\vec{X}(t) - \vec{X}(t)\right| \quad (4)$$

$$\vec{X}(t+1) = \vec{X}(t) - \vec{A}.D \quad (5)$$

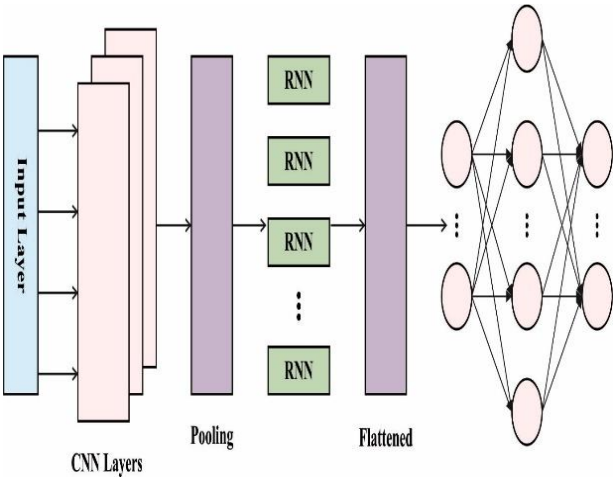

Fig. 2. Framework of CRNN.

Whereas $\vec{X}^*$ represents the best position of the attained solution, t characterizes the count of iterations, and the constant variables $\vec{A}$ and $\vec{C}$ are characterized by:

$$\vec{A} = 2\vec{a}.\vec{r} - \vec{a} \quad (6)$$

$$\vec{C} = 2.\vec{r} \quad (7)$$

Now, $\vec{r}$ denotes an arbitrary vector amongst [0, 1], and variable $\vec{a}$ is an arbitrary vector utilized for controlling the convergence procedure. It can be linearly decreased from two to zero through iteration:

$$\vec{a} = 2 - t\frac{2}{T} \quad (8)$$

In Eq. (5), t indicates the present iteration, and T shows the maximal iteration count of the vector $\vec{A}$ utilized for displaying the transition method amongst the exploratory and exploitative actions.

In WOA, the exploitation stage could be one of 2 models, shrinking surroundings or spiral-shaped methods. During the shrinking surrounding model, it is accomplished by reducing the value. The spiral path model upgrades the distance betwixt the most efficient search agents attained up to this point ($\vec{X}^*$) and searching agents (X), then boosts a novel location for the searching agent based on the subsequent as:

$$X(t+1) = D \cdot e^{bl}.\cos(2\pi l) + X^*(t) \quad (9)$$

The probabilities value of 0.5 is set as follows:

$$\vec{X}(t+1) = \begin{cases} D'.e^{bl}.\cos(2\pi l) + X^*(t), & p \geq 0.5 \\ \vec{X}(t) - \vec{A}.D, & p < 0.5 \end{cases} \quad (10)$$

Whereas p denotes an arbitrary probability value. The pseudocode of the proposed model is shown in Algorithm 1.

Algorithm 1: Overall process of WOADL-BDDC technique

Input: ADNI 3D Dataset
Output: Classified images
Start
For every image
do
Image_Pre-processing (GF_noise, U_Net skull stripping)
Segment_image()
QuickNAT mode
Hyperparameter adjustment using RMSProp Optimizer
End
Feature_extraction(radiomics)
Determine texture, shape, intensity
Classify()
Execute CRNN
Hyperparameter Tuning using WOA
Execute Exploration stage
Execute Exploitation stage
End
End

IV. Results and Discussion

The presented WOADL-BDDC system is simulated using a Python tool. The results are examined under the ADNI 3D dataset [22].

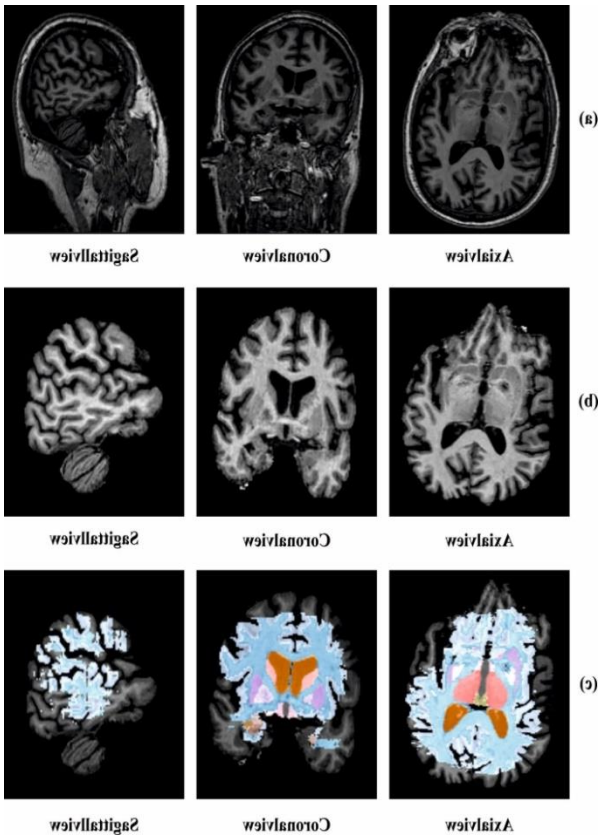

Fig. 3. (a) Original, (b) Pre-processed, (c) Segmented.

Fig. 3 visualization of the sample outcomes offered by the WOADL-BDDC system. Fig. 3(a) depicts the original brain MRI and the pre-processed image is provided in Fig. 3(b). Besides, the segmented images by the WOADL-BDDC system are shown in Fig. 3(c).

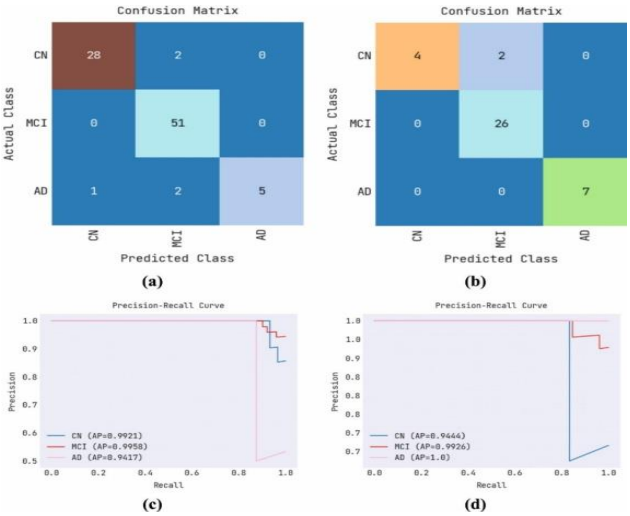

Fig. 4. (a) TR set confusion matrix (b) TS set confusion matrix (c) TR set PR-curve (d) TS set PR-curve.

Fig. 4 determines the classifier results of the WOADL-BDDC system under the training (TR) set and testing (TS) set. Fig. 4(a) represents the confusion matrix offered by the WOADL-BDDC model under the TR set. The figure symbolized that the WOADL-BDDC model had identified 28, 51, and 5 instances under CN, MCI, and AD classes. Also, Fig. 4(b) describes the confusion matrix offered by the WOADL-BDDC methodology under the TS set. The figure exemplified that the WOADL-BDDC algorithm has identified 4, 26, and 7 instances under CN, MCI, and AD classes. Fig. 4(c) and 4(d) validate the precision-recall analysis of the WOADL-BDDC system under training and TS sets. The figures described that the WOADL-BDDC method had acquired maximal precision-recall performance under all varying classes.

Table I reports the overall brain disorder classification outcomes of the WOADL-BDDC model. Fig. 5 represents a brief brain disorder classifier results of the WOADL-BDDC model under the TR set. The results indicated that the WOADL-BDDC model had shown enhanced results under all measures. It is noticed that the WOADL-BDDC model has gained an accuracy of 94.38%, percent of 96.43%, sense of 85.28%, species of 95.93%, $F1_{score}$ of 89.35%, and FPR of 4.07%.

TABLE I. Result Analysis of the WOADL-BDDC System with Distinct Measures

Metrics	TR set	TS set
Accuracy	94.38	94.87
Precision	96.43	97.62
Sensitivity	85.28	88.89
Specificity	95.93	94.87
F1-Score	89.35	92.10
False Positive Rate	04.07	05.13

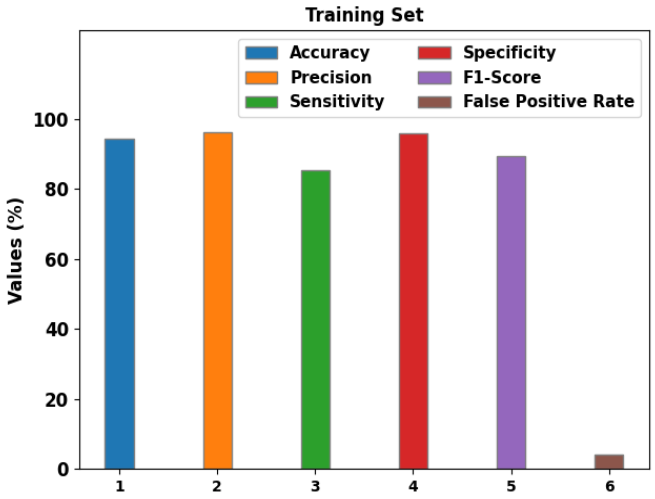

Fig. 5. Result in the analysis of the WOADL-BDDC system under the TR set.

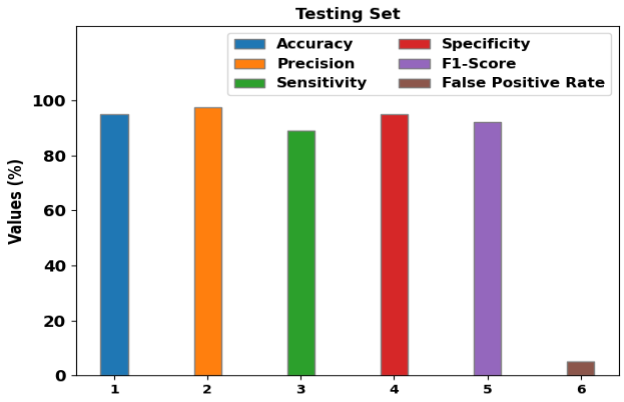

Fig. 6. Result in the analysis of the WOADL-BDDC system under the TS set.

Fig. 6 exemplifies a brief brain disorder classifier results of the WOADL-BDDC approach under the TS set. The outcomes referred that the WOADL-BDDC process has shown enhanced results under all measures. It is observed that the WOADL-BDDC system has gained an accuracy of 94.87%, percent of 97.62%, sense of 88.89%, species of 94.87%, $F1_{score}$ of 92.10%, and FPR of 5.13%.

An obvious ROC analysis of the WOADL-BDDC approach on the TR set is shown in Fig. 7. The outcomes referred to the WOADL-BDDC algorithm have exhibited their ability to categorize distinct classes.

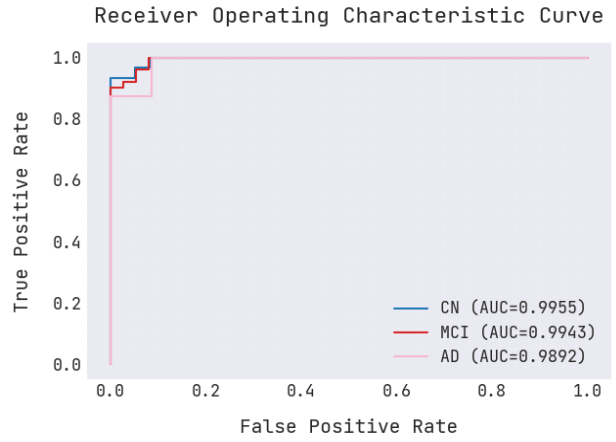

Fig. 7. ROC curve of WOADL-BDDC system under TR set.

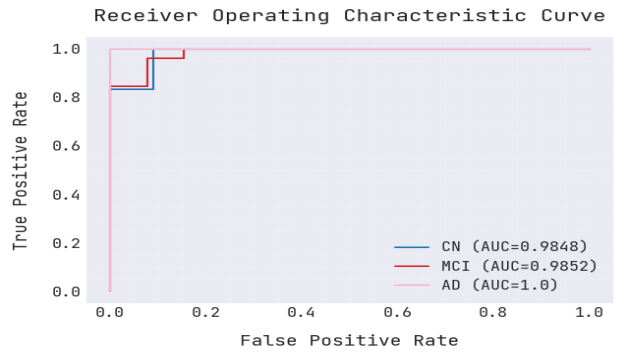

Fig. 8. ROC curve of WOADL-BDDC system under TS set.

A detailed ROC analysis of the WOADL-BDDC system on the TS set is displayed in Fig. 8. The outcomes stated the WOADL-BDDC approach had revealed its capability in varying classifier classes.

The training accuracy (TR_{acc}) and validation accuracy (VL_{acc}) acquired by the WOADL-BDDC system on the test database is depicted in Fig. 9. The simulation value stated that the WOADL-BDDC method had reached increased values of TR_{acc} and VL_{acc}. In particular, the VL_{acc} looked that greater than TR_{acc}.

The training loss (TR_{loss}) and validation loss (VL_{loss}) accomplished by the WOADL-BDDC system under the test database are displayed in Fig. 10. The simulation value pointed out that the WOADL-BDDC system has achieved lesser values of TR_{loss} and VL_{loss}. In particular, the VL_{loss} is lesser than TR_{loss}.

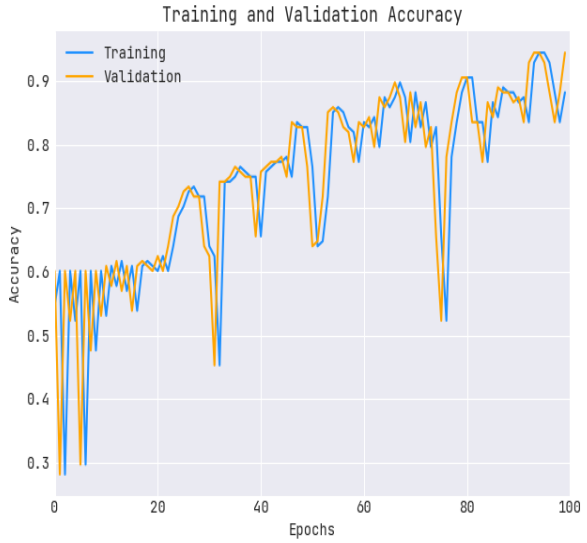

Fig. 9. Result analysis of WOADL-BDDC system in terms of TR_{acc} and VL_{acc}.

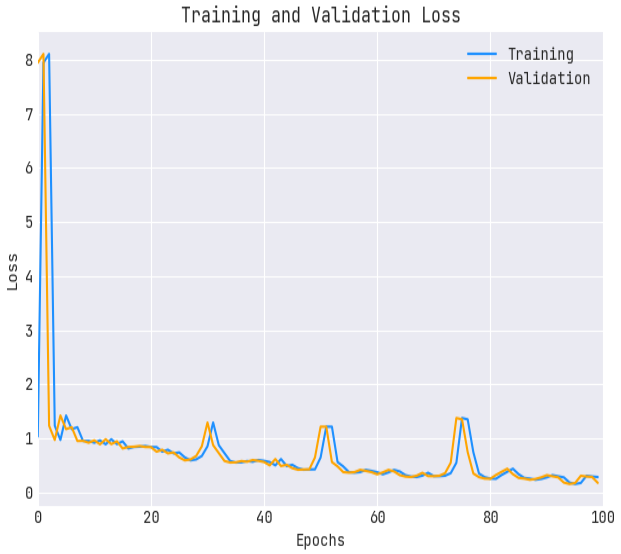

Fig. 10. Result Analysis of the WOADL-BDDC model in terms of TR_{loss} and VL_{loss}.

TABLE II. COMPARATIVE ANALYSIS OF THE WOADL-BDDC SYSTEM WITH RECENT SYSTEMS

Methods	Accuracy (%)	Specificity (%)
WOADL-BDDC	94.38	95.93
Vgg16	90.35	89.50
Graph CNN	94.00	93.02
Modified ResNet18	92.81	94.66
Non-linear SVM	75.58	75.63
ResNet50-SVM	92.49	87.36
ResNet50-RF	86.31	79.57

A comprehensive comparison study of the WOADL-BDDC model on brain disorder classification is shown in Table II [23, 24].

Fig. 11 represents a comparative investigation of the WOADL-BDDC technique with recent approaches in terms of accuracy. The results indicated that the non-linear SVM and ResNet50-RF models had attained the least accuracy values of 75.58% and 86.31%, respectively. Following, the VGG16 has shown a slightly enhanced accuracy of 90.35%. In contrast, the graph CNN, modified ResNet18, and ResNet50-SVM models have reached reasonable accuracy values of 94%, 92.81%, and 92.49%. Finally, the WOADL-BDDC model has obtained promising performance with a higher accuracy of 94.38%.

Fig. 12 signifies a comparative investigation of the WOADL-BDDC system with current methods in terms of species. The outcomes indicated that the non-linear SVM and ResNet50-RF approaches had correspondingly accomplished the least $spec_y$ values of 75.63% and 79.57%. Next, the VGG16 has demonstrated a somewhat improved $spec_y$ of 89.50%. In contrast, the graph CNN, modified ResNet18, and ResNet50-SVM models have reached reasonable $spec_y$ values of 93.02, 94.66%, and 87.36%. Finally, the WOADL-BDDC methodology has attained promising performance with a higher $spec_y$ of 95.93%.

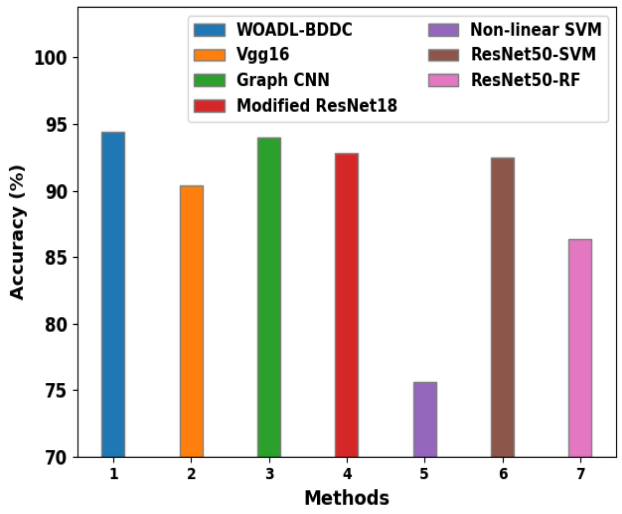

Fig. 11. $Accu_y$ analysis of WOADL-BDDC system with recent algorithms.

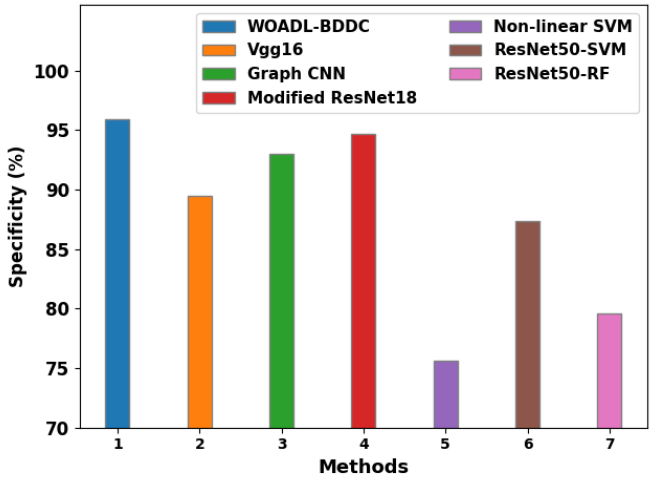

Fig. 12. $Spec_y$ analysis of WOADL-BDDC system with recent algorithms.

These results confirmed the automated and accurate brain disorder classification results of the WOADL-BDDC model.

V. CONCLUSION

In this study, we have established a novel WOADL-BDDC technique for recognizing brain disorders on MRI images. Primarily, the presented WOADL-BDDC technique performs pre-processing in two stages: GF-based noise elimination and U-Net segmentation-based skull stripping. Besides, the QuickNAT with RMSProp optimizer is applied to segment the brain parts. For feature extraction, the WOADL-BDDC technique performs a radiomics approach that separates features of all aspects. Finally, WOA with CRNN model is applied for brain disorder classification. The experimental evaluation of the WOADL-BDDC technique is tested on ADNI 3D dataset. The comprehensive comparison study highlighted the adequate performance of the WOADL-BDDC technique in different measures. In the future, an ensemble of DL-based classifiers can be employed to improve the WOADL-BDDC technique's detection performance.

VI. FUNDING STATEMENT

The authors received no specific funding for this study.

VII. CONFLICTS OF INTEREST

The authors declare they have no conflicts of interest to report regarding the present study.

REFERENCES

[1] AlSaeed, D.; Omar, S.F. Brain MRI Analysis for Alzheimer's Disease Diagnosis Using CNN-Based Feature Extraction and Machine Learning. Sensors , 22, 2911,2022. https://doi.org/10.3390/s22082911.

[2] Altaf, T., Anwar, S.M., Gul, N., Majeed, M.N. and Majid, M., Multi-class Alzheimer's disease classification using image and clinical features. *Biomedical Signal Processing and Control*, *43*, pp.64-74,2018.

[3] Alwajih, R., Abdulkadir, S.J., Al Hussian, H., Aziz, N., Al-Tashi, Q., Mirjalili, S. and Alqushaibi, A., Hybrid binary whale with harris hawks for feature selection. *Neural Computing and Applications*, pp.1-19,2022.

[4] An, N., Ding, H., Yang, J., Au, R. and Ang, T.F. Deep ensemble learning for Alzheimer's disease classification. *Journal of biomedical informatics*, *105*, pp.103-112,2020.

[5] Basheera, S. and Ram, M.S.S.,Convolution neural network–based Alzheimer's disease classification using hybrid enhanced independent component analysis based segmented gray matter of T2 weighted magnetic resonance imaging with clinical valuation. *Alzheimer's & Dementia: Translational Research & Clinical Interventions*, *5*, pp.974-986,2019.

[6] Bi, X. and Wang, H., Early Alzheimer's disease diagnosis based on EEG spectral images using deep learning. *Neural Networks*, *114*, pp.119-135,2019.

[7] Fouad, A., Moftah, H. M., &Hefny, H. A., Brain diagnoses detection using whale optimization algorithm based on ensemble learning classifier. Int. J. Intell. Eng. Syst, 13(2), 40-51,2020.

[8] Hu, Y., Wen, C., Cao, G., Wang, J. and Feng, Y., Brain network connectivity feature extraction using deep learning for Alzheimer's disease classification. *Neuroscience Letters*, *782*, p.136673.2022.

[9] Jo, T., Nho, K., Bice, P., Saykin, A.J. and Alzheimer's Disease Neuroimaging Initiative, Deep learning-based identification of genetic variants: application to Alzheimer's disease classification. *Briefings in Bioinformatics*, *23*(2), p.bbac022,2022.

[10] Jo, T., Nho, K., Risacher, S.L. and Saykin, A.J., Deep learning detection of informative features in tau PET for Alzheimer's disease classification. *BMC bioinformatics*, *21*(21), pp.1-13,2020.

[11] Arulananth, T.S., Balaji, L., Baskar, M. , PCA Based Dimensional Data Reduction and Segmentation for DICOM Images. *Neural Process Lett* 2020. https://doi.org/10.1007/s11063-020-10391-9.

[12] Khagi, B., Kwon, G.R. and Lama, R., Comparative analysis of Alzheimer's disease classification by CDR level using CNN, feature selection, and machine-learning techniques. *International Journal of Imaging Systems and Technology*, *29*(3), pp.297-310.,2019.

[13] Khan, M.A., HCRNNIDS: hybrid convolutional recurrent neural network-based network intrusion detection system. *Processes*, *9*(5), p.834,2021.

[14] Li, L. and Ma, H., Pulse coupled neural network-based multimodal medical image fusion via guided filtering and WSEML in NSCT domain. *Entropy*, *23*(5), p.591,2021.

[15] Liang, G., Xing, X., Liu, L., Zhang, Y., Ying, Q., Lin, A.L. and Jacobs, N., Alzheimer's disease classification using 2d convolutional neural networks. In *2021 43rd Annual International Conference of the IEEE Engineering in Medicine & Biology Society (EMBC)* (pp. 3008-3012). IEEE,2021.

[16] Odusami, M.; Maskeliunas, R.; Damasevicius, R.; Krilavicius, T. Analysis of Features of Alzheimer's Disease: Detection of Early Stage from Functional Brain Changes in Magnetic Resonance Images Using a Finetuned ResNet18 Network. Diagnostics 2021, 11, 1071. https:// doi.org/10.3390/diagnostics11061071.

[17] Qiu, S., Joshi, P.S., Miller, M.I., Xue, C., Zhou, X., Karjadi, C., Chang, G.H., Joshi, A.S., Dwyer, B., Zhu, S. and Kaku, M., Development and validation of an interpretable deep learning framework for Alzheimer's disease classification. *Brain*, *143*(6), pp.1920-1933,2020.

[18] Roy, A.G., Conjeti, S., Navab, N., Wachinger, C. and Alzheimer's Disease Neuroimaging Initiative, QuickNAT: A fully convolutional network for quick and accurate segmentation of neuroanatomy. *NeuroImage*, *186*, pp.713-727,2019.

[19] Sampath, R. and Baskar, M., 3D brain image-based Alzheimer's disease detection techniques using fish swarm optimizer's deep convolution Siamese neural network. Expert Systems, p.e12963,2022.

[20] Shanmugam, J.V., Duraisamy, B., Simon, B.C. and Bhaskaran, P., Alzheimer's disease classification using pre-trained deep networks. *Biomedical Signal Processing and Control*, *71*, p.103217,2022.

[21] Sharma, R., Goel, T., Tanveer, M. and Murugan, R.,. FDN-ADNet: Fuzzy LS-TWSVM based deep learning network for prognosis of the Alzheimer's disease using the sagittal plane of MRI scans. *Applied Soft Computing*, *115*, p.108099,2022.

[22] Tian, J., Smith, G., Guo, H., Liu, B., Pan, Z., Wang, Z., Xiong, S. and Fang, R. Modular machine learning for Alzheimer's disease classification from retinal vasculature. *Scientific Reports*, *11*(1), pp.1-11,2021.

[23] Wang, Y., Liu, W., Yu, Y., Liu, J.J., Xue, H.D., Qi, Y.F., Lei, J., Yu, J.C. and Jin, Z.Y.,CT radiomics nomogram for the preoperative prediction of lymph node metastasis in gastric cancer. *European radiology*, *30*(2), pp.976-986,2020.

[24] Zhang, J., Zheng, B., Gao, A., Feng, X., Liang, D. and Long, X., A 3D densely connected convolution neural network with connection-wise attention mechanism for Alzheimer's disease classification. *Magnetic Resonance Imaging*, *78*, pp.119-126,2021.

[25] Amin, J., Sharif, M., Haldorai, A., Yasmin, M., and Nayak, R. S. , Brain tumor detection and classification using machine learning: a comprehensive survey. Complex Intell. Syst. 8, pp.3161–3183,2021. doi: 10.1007/s40747-021-00563-y.

[26] Baskar, M., Renuka Devi, R., Ramkumar, J. , Region Centric Minutiae Propagation Measure Orient Forgery Detection with Finger Print Analysis in Health Care Systems. *Neural Process Lett* . 2021. https://doi.org/10.1007/s11063-020-10407-4.

[27] Houssein, E. H., Ibrahim, I. E., Neggaz, N., Hassaballah, M., and Wazery, Y. M. , An efficient ecg arrhythmia classification method based on manta ray foraging optimization. Expert. Syst. Appl. 181, 115131,2021. doi: 10.1016/j.eswa.2021.115131.

[28] Bekhet, S., Hassaballah, M., Kenk, M. A., and Hameed, M. A. , An artificial intelligence based technique for COVID-19 diagnosis from chest x-ray, in 2020 2nd Novel Intelligent and Leading Emerging Sciences Conference (NILES) (Giza: IEEE), pp.191–195,2020.